

RECENT COMMISSIONING EXPERIENCE OF THE FERMI@ELETTRA FIRST BUNCH COMPRESSOR AREA: INVESTIGATIONS OF BEAM DYNAMICS, MODELING AND CONTROL SOFTWARE

S. Di Mitri[#], E. Allaria, R. Appio, L. Badano, G. De Ninno, D. Castronovo, M. Cornacchia, P. Craievich, S. Ferry, L. Frolich, A. Lutman, G. Penco, C. Scafuri, S. Spampinati, C. Spezzani, M. Trovò, M. Veronese, S. V. Milton, Sincrotrone Trieste (ELETTRA), Trieste, Italy
 R. Bartolini, DLS Ltd, Oxford, U.K.
 P. Evthushenko, JLAB, Newport News, VA 23606, U.S.A.
 W. Fawley, LBNL, Berkeley, CA 94704, U.S.A.
 L. Giannessi, ENEA, Frascati, Italy
 M. Sjoström, MAX-lab, Lund, Sweden

Abstract

Measurements have recently been collected from the FERMI@elettra Free Electron Laser first bunch compressor area. This region includes a magnetic compressor, diagnostics for the characterization of the longitudinal and transverse phase space and suitable optics for matching to the downstream part of the linac. We report on the beam dynamics investigations in comparison with the modeling as well as the high level software control that was essential in making these measurements.

INTRODUCTION

FERMI@elettra is an S-band linac-based Free Electron Laser (FEL) implementing High Gain Harmonic Generation (HG) in the 100–4 nm output wavelength range [1,2]. Commissioning started in September 2009 [3] and first light will provide to the user facility at the beginning of 2011. The linac layout is shown in Figure 1.

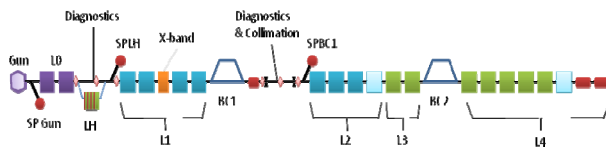


Figure 1: Split schematic of FERMI@elettra: accelerating sections (Gun, L0–L4), compressors (BC1, BC2).

The first commissioning of the FERMI@elettra magnetic compressor BC1 was carried out over a 4 weeks period in July 2010. At the same time, a refinement of the machine performance and beam dynamics in the upstream linac was performed. During the final week of this period, the beam was passed through the entire linac and sent to the beam dump at the end of it. Major goals were achieved in terms of comparison of the machine model with the measured quantities. The good correspondence between the model and measured quantities has translated into online control of the accelerator optics matching, trajectory correction and bunch length compression. Some unexpected effects on the beam dynamics have been observed such spurious dispersion, transverse wake field

effects and emittance growth due to chromatic effects in the BC1 area. These perturbations will be further studied and fixed in the next runs.

MEASUREMENTS VS. MODEL

Table 1: Electron beam parameters up to the BC1 area. Measurement results vs. model prediction.

Parameter	Model	Measurement
Charge [pC]	250	250 – 220 ± 20
Charge jitter, rms [%]	<4	0.5
PI laser radius [mm]	0.7	0.7
PI pulse length, FW [ps]	5.0	5.0 ± 0.1
Bunch duration, FW [ps]	6.0	6.0 ± 0.5
Norm. transv. proj. emittance (H,V) [mm mrad]	0.8, 0.8	0.88(G)/1.04(C)±0.1 1.25(G)/1.23(C)±0.1
Mismatch in LH area (H,V)	1.0, 1.0	1.005 ± 0.003, 1.001 ± 0.002
Mismatch in BC1 area (H,V)	1.0, 1.0	1.030 ± 0.004, 1.117 ± 0.124
Gun <E> (working phase) [MeV]	5.0	4.5 – 4.9 ± 0.01
Total Energy Spread out of Gun, rms [keV]	40	28 – 44 ± 5
<E> out of L0 (on-crest) [MeV]	96	97.25 ± 0.05
Total Energy Spread out of L0, rms [keV]	45	43 – 51 ± 1
<E> out of L1 (on-crest) [MeV]	345	357.6 ± 0.05
Total Energy Spread out of L1, rms [keV]	200	≥ 135 ± 1
<E> jitter out of Gun (working phase, rms [keV])	< 5	6 ± 1
<E> jitter out of L0 (on-crest), rms [keV]	< 9.6	9 ± 1
<E> jitter out of L1 (-20deg out of crest), rms [keV]	< 300	< 660 ± 1
<E> stab. over 6hs out of L1 (on-crest, p-to-p) [MeV]	< 0.3	1.0 ± 0.05
Energy Spread stab. over 6hs out of L1 (on-crest, p-to-p) [keV]	< 0.3	0.15 ± 0.01
Trajectory jitter, (rms) [μm]	< 20	30

[#]simone.dimitri@elettra.trieste.it

Table 1 lists the electron beam parameters measured *before* compression and compares them with the exact model prediction (see next Sections for details).

CHARGE EXTRACTION

The beam charge has been transported with 100% efficiency from the Gun to the BC1 spectrometer line. The copper cathode quantum efficiency (QE) has suffered from a progressive degradation, as shown in Figure 2. However, the projected emittance measurement does not reveal any obvious correlation with that. QE recovers following an in-house developed cleaning method [4].

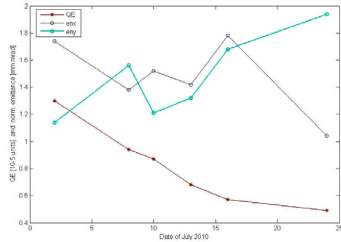


Figure 2: QE (in units of 10^{-5}) and normalized emittances measured in the same dates during July 2010.

INITIAL BUNCH DURATION

The bunch length has been measured with two independent methods. In one method, a Cherenkov detector inserted in the straight line out of the Gun [3] indicates a 6 ps long bunch. Using a second method, the horizontal beam size Δx measured at the screen in the BC1 spectrometer line (SPBC1) with on-crest acceleration in L1 related to the full-width bunch length Δz and the local dispersion function η :

$$\Delta z_{pk-to-pk} = \frac{\lambda_{RF}}{\pi} \arccos\left(\frac{\Delta x}{\eta} - 1\right) \quad (1)$$

The assumption of a beam symmetrically distributed across the RF crest has been verified thanks to an occasional vertical deflection observed at the screen, that generates a half-moon shape in the (x,y) plane (see Figure 5). The measurement error is dominated by the mean energy jitter providing an uncertainty on the bunch length in the range of 5.7-6.2 ps. The Cherenkov detector, the on-crest RF phase technique and simulation results using the Astra code [5], using the laser and parameters in Table 1, are in full agreement.

OPTICS MATCHING AND TRANSPORT

The beam optics matching is performed with the *elegant* code [6] interfaced to the Tango server through Matlab scripts. Beam size measurements are taken, magnet settings are read, matching is computed by the code and this is finally applied to the machine. The experimental mismatch parameter $B_{mag} = 0.5(\beta_{meas}\gamma_{th} - 2\alpha_{th}\alpha_{meas} + \beta_{th}\gamma_{meas}) \geq 1$ confirms the beam optics is matched in 2 or 3 iterations. A good week-by-week reproducibility of the machine optics is also

confirmed. Once the optics is matched in the LH area (~ 95 MeV), the beam is simply transported to the BC1 area (~ 345 MeV) with the correct optics with good results (see the mismatch parameter in Table 1). Note: also included in the model are the BC1 dipole magnets vertical focusing and cavity end RF focusing (compare middle and bottom plot in Figure 3).

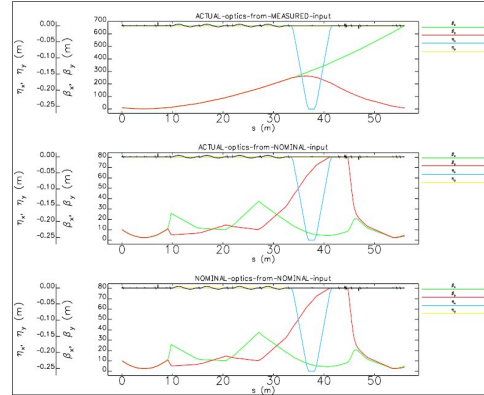


Figure 3: Top, current optics. Middle, predicted optics after matching. Bottom, model.

TRAJECTORY CORRECTION

The pre-existing Matlab application for trajectory feedback was further developed during the run by adding support for non-square response matrices of low rank, capability to import theoretical response matrices from the *elegant* code, as well as visualization of response matrices and their pseudo-inverse (see Figure 4). The problem of low-rank matrices was handled using singular value decomposition and a manipulation of the singular values, either by truncation of small values or by Tikhonov regularization [7]. Attempts to correct the trajectory using the theoretical response matrix up to and including BC1 were successful.

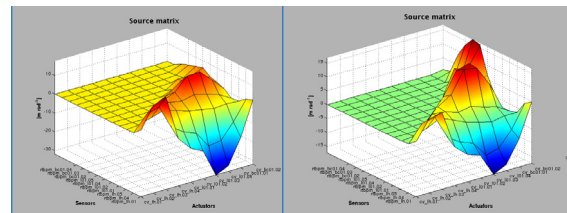


Figure 4: Measured (left) and theoretical (right) trajectory response matrix from the LH area to SPBC1 (13 correctors per plane and 11 BPMs)

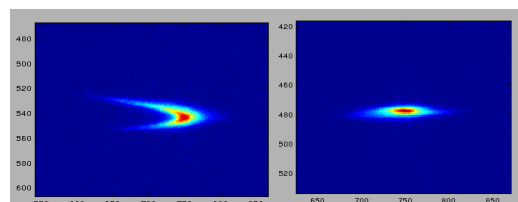


Figure 5: Beam image at the screen in SPBC1 A vertical deflection (top) reveals the on-crest acceleration in L1. It is canceled by a trajectory bump in L1 (bottom) calculated with the theoretical response matrix.

Even when starting from 2 mm displacements at some locations, the trajectory converges well to the 50 μm level over all BPMs in a pair of seconds. Feedback is used to maintain the desired trajectory and also to create closed bumps along L1 to compensate for an unwanted vertical deflection observed at SPBC1 (see Figure 5).

DISPERSION MEASUREMENT

The dispersion function along the FERMI linac was measured by changing the RF voltage applied to the two accelerating sections of L1 and monitoring the trajectory changes downstream (see Figure 6). Initial measurements show that the dispersion function is non zero along the linac in both planes, possibly as a result of a spurious dispersion at the linac entrance. The effect of the bunch compressor on the dispersion function was also measured by scanning the compressor strength, as shown in Figure 7. The agreement with the model is satisfactory at these early stages. The dispersion bump introduced by the BC1 magnetic chicane is reasonably well closed after the 4th dipole and, for a bending angles up to 0.12 rad (the nominal value is 0.085rad), the residual trajectory distortion remains within the 10 μm level at the two BPMs downstream of BC1. The bend magnets trim coils correct the trajectory to the level of 20 μm . These correct for the magnet-to-magnet differences that could in principle corrupt the achromaticity of the chicane.

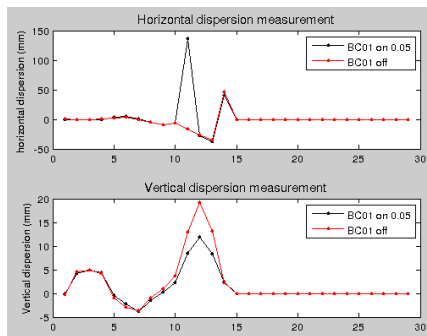


Figure 6: Dispersion function from the LH to BC1 area. A factor of 1/4 has to be applied from abscissa equal to 10 and downstream because of a wrong scaling in the script.

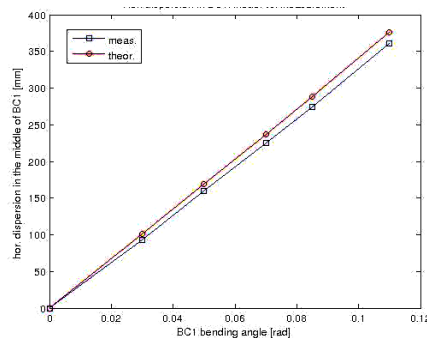


Figure 7: Dispersion function in the middle of BC1 vs. bending angle.

PHASE SPACE RECONSTRUCTION

The electron beam transverse phase space has been reconstructed both in the LH and in the BC1 diagnostic straight line (see Table 2 and 3) with tomographic technique [8] by using three succeeding screens separated by 120° total betatron phase advance. Five measurements are used for an estimation of the uncertainty on the measured central value. Figure 8 shows a typical phase space reconstruction in the LH area.

Table 2: Projected normalized emittances measured in LH and in BC1 area.

	Quad-scan	Tomography
$\epsilon_{n,x}$ [mm mrad] in LH	1.8 ± 0.2	2.0 ± 0.05
$\epsilon_{n,y}$ [mm mrad] in LH	2.1 ± 0.2	2.0 ± 0.10
$\epsilon_{n,x}$ [mm mrad] in BC1	3.9 ± 0.5	4.0 ± 0.4
$\epsilon_{n,y}$ [mm mrad] in BC1	4.0 ± 0.5	2.8 ± 0.1

Table 3: Twiss parameters measured in LH and BC1 area.

	Quad-scan	Tomography	Model
β_x [m] in LH	11.7 ± 0.2	11.8 ± 0.2	10.174
β_y [m] in LH	11.2 ± 0.4	8.2 ± 0.3	10.174
α_x in LH	1.7 ± 0.1	1.6 ± 0.1	1.732
α_y in LH	1.7 ± 0.1	0.8 ± 0.3	1.732
β_x [m] in BC1	12.8 ± 0.7	13.3 ± 1.3	11.186
β_y [m] in BC1	19.5 ± 0.4	19.6 ± 0.6	10.186
α_x in BC1	1.7 ± 0.1	1.0 ± 0.1	1.732
α_y in BC1	1.7 ± 0.1	1.4 ± 0.1	1.732

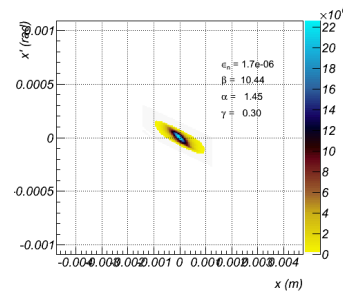


Figure 8: Typical reconstruction of the horizontal transverse phase space at the first screen of 3 in the LH area, for a beam optics close to the model.

BUNCH LENGTH MONITOR

A bunch length monitor [9] is installed downstream of BC1. It is based on the detection of the edge radiation coming from the last dipole of BC1 and the diffraction radiation coming from a ceramic gap. The coherent edge radiation is detected by a pyrodetector, while gap radiation is collected by 3 electromagnetic horns, and detected by 3 RF diodes operating at the 30 GHz, 100 GHz and 300 GHz bands. The relative bunch length measurement obtained in this way will be used in the longitudinal feedback system. The 3 diodes show relative rms noise of values under 2% with 0.5% for the 30 GHz diode, while the pyrodetector SNR is around 10%. The source of this difference is still under investigation. A

comparison of measurements with the theory for gap radiation emission [10] has been performed showing excellent agreement of the signal vs. linear compression factor and good reproducibility of the measured signal.

EMITTANCE STUDIES WITH BC1

The projected emittance has been measured in “slow” [3] and “real-time” mode. In real-time mode, during the quadrupole scan, the quadrupole settings are related to the bunch number at 10 Hz repetition rate. This option is extremely useful for fast emittance optimization or emittance scan vs. another machine parameter, i.e. gun solenoid strength or trajectory correction at low energy.

The emittance values reported in this paper have been measured using 100% of the image at the screen, after noise subtraction. The OTR screen always gives a lower emittance value than YAG because of its higher resolution. We have verified that the Gaussian (G) distribution, applied to the beam images collected at the screens, usually ignores some halo tails but works well for the optics matching. Alternatively, the *confiteor* (C) 2-D fitting function [3] usually fits well 100% of the particle distribution and it is more reliable for a correct computation of the projected emittance. G and C fitting techniques converge to the same emittance value after optics matching is good.

The bunch length compression is controlled with the panel in Figure 9 where user variables are: chicane bending angle (mechanical mover of the vacuum chamber), current supplying the dipole magnets, L1 RF phase and voltage. Calibration tables automatically supply the dipole magnet currents according to the chicane bending angle, for any linac setting; they also cancel the 1st and 2nd integral of the chicane with the 4 trim coils.

The projected emittance, routinely measured in the LH area in the range 1.2–1.7 mm mrad, is degraded after passing through L1. Figure 11 shows the horizontal emittance as function of the L1 RF phase (0 is on-crest) with BC1 off and at 0.085 rad bending angle, respectively. By virtue of the large residual dispersion in this region (see Figure 6), chromatic aberrations could explain the growth with no compression as the energy chirp increases (same in the vertical plane). However, with BC1 off the emittance reaches a minimum of 1.45 mm mrad for -15 RF phase (not shown here). Further investigations are needed to understand these observations.

A contribution from coherent synchrotron radiation is suspected from the fast increase of the curves for $CF \geq 3.2$ (phase ≥ 20 deg). *elegant* simulations predict ~15% emittance growth only for $CF \geq 10$. Owing to the non-linearized longitudinal phase space at the entrance of BC1, it also predicts a ~1kA, ~20fs current spike at the bunch head for $CF \geq 3$. If the slice optics of the spike is not well matched to the lattice, then this could be the natural source of the projected emittance blow up shown in Figure 10. Figure 11 shows the beam image at the 2nd screen downstream of BC1. The fragmented image

reaching saturation of the screen system can be interpreted as COTR. This effect disappears with the YAG target or by inserting an OTR foil upstream of it.

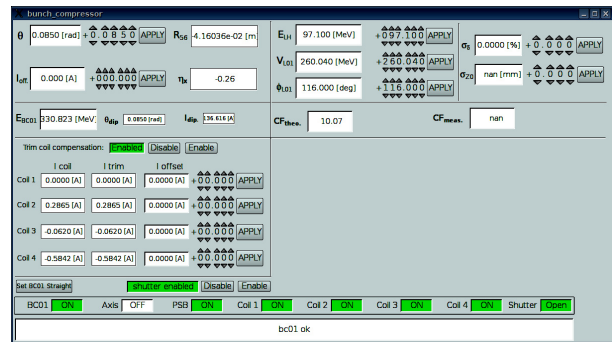


Figure 9: BC1 control panel.

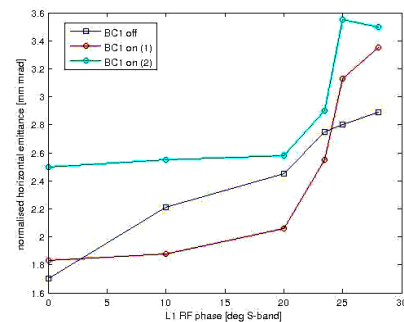


Figure 10: Normalized horizontal emittance in BC1 area, with and without compression. The error on the central values is of the order of 10%.

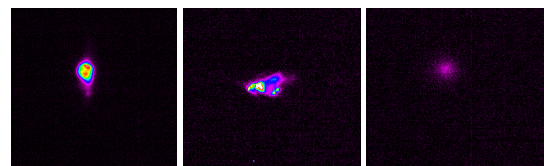


Figure 11: Beam image at the screen downstream of BC1 for $CF=4$. Left, YAG target ($137H \times 148V \mu\text{m rms}$). Center, OTR target ($511H \times 154V \mu\text{m rms}$). Right, OTR target after insertion of an upstream OTR foil ($527H \times 413V \mu\text{m rms}$).

REFERENCES

- [1] C. Bocchetta et al., FERMI@Elettra CDR (2007).
- [2] S. Di Mitri et al., NIM A **608** (2009), 19–27.
- [3] G. Penco et al., Proc. of IPAC 2010, TUOARA02, Kyoto, Japan.
- [4] M. Trovo³, private communications.
- [5] K. Flöttman, <https://www.desy.de/~mpyflo/>
- [6] M. Borland, APS LS-287, 2000.
- [7] A.N.Tikhonov, Doklady Akademii Nauk SSSR, 39(5):195-198 (1943).
- [8] F. Lohl, TESLA-FEL 2005-03 (2005).
- [9] M. Veronese et al., this conference.
- [10] L. Palumbo, CERN-LEP-TH/84-4 (1984).